MOLECULAR ECOLOGY

Molecular Ecology (2015) **24**, 5864–5876 doi: 10.1111/mec.13440

Spatiotemporal analysis of gene flow in Chesapeake Bay Diamondback Terrapins (*Malaclemys terrapin*)

PAUL E. CONVERSE,* SHAWN R. KUCHTA,*† WILLEM M. ROOSENBURG,*† PAULA F. P. HENRY,‡ G. MICHAEL HARAMIS‡ and TIM L. KING§

*Department of Biological Sciences, Ohio University, Athens, OH 45701, USA, †Ohio Center for Ecology and Evolutionary Studies, Ohio University, Athens, OH 45701, USA, ‡U.S. Geological Survey, Patuxent Wildlife Research Center, BARC-East, Building 308, 10300 Baltimore Avenue, Beltsville, MD 20705, USA, §U.S. Geological Survey, Leetown Science Center, Aquatic Ecology Laboratory, 11649 Leetown Road, Kearneysville, WV 25430, USA

Abstract

There is widespread concern regarding the impacts of anthropogenic activities on connectivity among populations of plants and animals, and understanding how contemporary and historical processes shape metapopulation dynamics is crucial for setting appropriate conservation targets. We used genetic data to identify population clusters and quantify gene flow over historical and contemporary time frames in the Diamondback Terrapin (*Malaclemys terrapin*). This species has a long and complicated history with humans, including commercial overharvesting and subsequent translocation events during the early twentieth century. Today, terrapins face threats from habitat loss and mortality in fisheries bycatch. To evaluate population structure and gene flow among Diamondback Terrapin populations in the Chesapeake Bay region, we sampled 617 individuals from 15 localities and screened individuals at 12 polymorphic microsatellite loci. Our goals were to demarcate metapopulation structure, quantify genetic diversity, estimate effective population sizes, and document temporal changes in gene flow. We found that terrapins in the Chesapeake Bay region harbour high levels of genetic diversity and form four populations. Effective population sizes were variable. Among most population comparisons, estimates of historical and contemporary terrapin gene flow were generally low ($m \approx 0.01$). However, we detected a substantial increase in contemporary gene flow into Chesapeake Bay from populations outside the bay, as well as between two populations within Chesapeake Bay, possibly as a consequence of translocations during the early twentieth century. Our study shows that inferences across multiple time scales are needed to evaluate population connectivity, especially as recent changes may identify threats to population persistence.

Keywords: conservation genetics, contemporary gene flow, historical gene flow, metapopulation, population admixture, population structure, translocation

Received 20 April 2015; revision received 26 October 2015; accepted 27 October 2015

Introduction

The current genetic structure among a set of populations is the product of contemporary and historical processes, and distinguishing between the two is paramount for effective population management. Around the world, the fragmentation of habitats is a ubiquitous threat to biodiversity because it decreases population connectivity (dispersal and gene flow) relative to historical levels, thereby impacting metapopulation dynamics (Hanski & Gilpin 1997; Frankham *et al.* 2002). Reductions in gene flow and small effective population size (N_e) caused by habitat fragmentation diminish metapopulation viability by decreasing genetic diversity and increasing inbreeding (Lande 1995; Templeton *et al.*

Correspondence: Paul E. Converse, Fax: +1 740 593 0300, E-mail: paulconverse@icloud.com

2001; Bowler & Benton 2005; Epps *et al.* 2005; Banks *et al.* 2013; Barr *et al.* 2015). The extent to which habitat fragmentation decreases population connectivity, however, is dependent upon the interaction between landscape features and organismal dispersal behaviour (Gu *et al.* 2002; Caizergues *et al.* 2003; Braunisch *et al.* 2010; Callens *et al.* 2011; Crispo *et al.* 2011; Castillo *et al.* 2014). In many cases, populations that are currently isolated by habitat fragmentation may not have been isolated in the past (Newmark 2008; Chiucchi & Gibbs 2010; Epps *et al.* 2013; Husemann *et al.* 2015). In contrast to habitat fragmentation, the anthropogenic translocation of individuals between populations reduces genetic differentiation, increases diversity within populations and may obscure estimates of genetic connectivity (Templeton *et al.* 1986; Moritz 1999; Weeks *et al.* 2011). Disentangling how historical and contemporary processes affect current patterns of genetic diversity is a formidable challenge, but can be achieved by temporal sampling (Husemann *et al.* 2015), or by separately estimating contemporary and historical processes (Chiucchi & Gibbs 2010; Epps *et al.* 2013).

In this article, we examine population structure and connectivity in the Diamondback Terrapin (*Malaclemys terrapin*). Terrapins inhabit North American coastal and brackish waters, with a range that extends from Texas to Massachusetts (Ernst & Barbour 1989). During the nineteenth and early twentieth centuries, terrapins were unsustainably harvested, resulting in severe population contractions and local extirpations (Garber 1988; Garber 1990). To help preserve dwindling populations and supplement terrapin harvests, governmental and private entities constructed terrapin breeding farms (Coker 1906; Barney 1924; Hildebrand & Hatsel 1926; Hildebrand 1929). Terrapins from Chesapeake Bay were the preferred variety for consumption (Hay 1917; Hildebrand 1929), and the demand for 'Chesapeakes' resulted in terrapins from North Carolina and possibly other populations to be imported into Chesapeake Bay terrapin farms (Coker 1920). Terrapin meat eventually fell out of favour, and as breeding farms closed, terrapins were reportedly released into local waters. The amount of admixture from these translocated terrapins is unknown.

While terrapin harvesting in Maryland has been discontinued (Roosenburg *et al.* 2008), terrapins still face a myriad of threats, including mortality from boat strikes (Roosenburg 1991; Cecala *et al.* 2008), drowning in crab and eel pots (Roosenburg *et al.* 1997; Radzio & Roosenburg 2005; Dorcas *et al.* 2007; Grosse *et al.* 2009), habitat loss and fragmentation (Roosenburg 1991; Wood & Herlands 1997) and predator introductions (Feinberg & Burke 2003). As male terrapins are smaller and disperse longer distances than do females (Sheridan 2010), they are particularly vulnerable to dispersal-related mortality. Terrapin populations in Chesapeake Bay exhibit highly skewed sex ratios in favour of females (Roosenburg 1991; W. Roosenburg unpublished data), making successful male dispersal important for maintaining genetic connectivity.

The consequences of habitat fragmentation and increased mortality on connectivity and population genetic structure are not entirely clear, however, and ecological and molecular findings are discordant with respect to levels of connectivity (Converse & Kuchta *in press*). Ecological data show terrapins reside in small home ranges of 0.54–3.05 km^2 (Spivey 1998; Butler 2002) and can remain in the same study site for over a decade (Lovich & Gibbons 1990; Gibbons *et al.* 2001). Furthermore, ecological data suggest terrapins form structured breeding assemblages, with females returning to the same nesting beach each season (Auger 1989; Roosenburg 1994; Mitro 2003) and hatchlings demonstrating natal philopatry (Sheridan *et al.* 2010). In contrast to these studies, genetic studies indicate that terrapin populations are weakly differentiated (Hart *et al.* 2014), with limited structure at both regional and local scales (Hauswaldt & Glenn 2005; Sheridan *et al.* 2010; Glenos 2013; Drabeck *et al.* 2014; Petre 2014).

The complex history terrapins share with humans in Chesapeake Bay makes it important to quantify levels of population genetic structure, including a comparison of contemporary and historical levels of connectivity. In this article, we report on a study of metapopulation dynamics of the Diamondback Terrapin in Chesapeake Bay. Specifically, we estimate the following: (i) the number of genetic populations in Chesapeake Bay; (ii) levels of genetic diversity within and among populations; (iii) effective population sizes; and (iv) levels of contemporary and historical gene flow among populations. In addition, we identify possible instances of terrapin translocation. By comparing historical and contemporary levels of genetic connectivity, we examine the impact of habitat fragmentation and population translocations on patterns of genetic variation, and help resolve the discordance between ecological and molecular studies (Converse & Kuchta *in press*).

Materials and methods

Sampling localities and microsatellite genotyping

We sampled 617 terrapins from 15 localities throughout Chesapeake Bay and nearby coastal bays between 2003 and 2005 (Fig. 1; Appendix S1, Supporting Information). Terrapins were captured using fyke nets or collected in winter refugia during hibernation (Haramis *et al.* 2011). Terrapins were marked with passive integrated

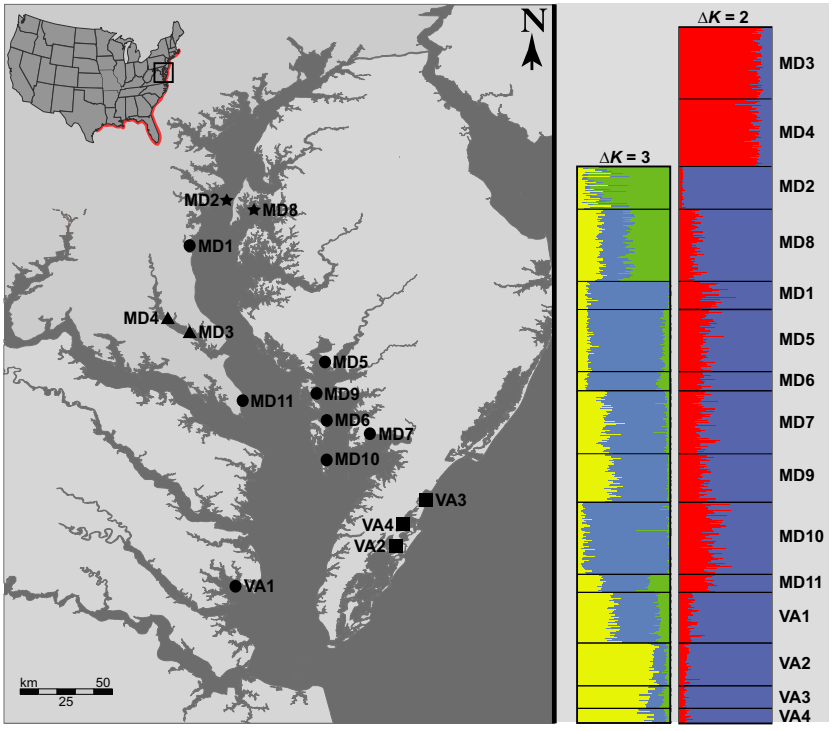

Fig. 1 Sampling localities and STRUCTURE results. Top left: the distribution of Diamondback Terrapins (shaded red), and the location of the study (black box). Main figure: four terrapin populations were demarcated. Triangles indicate the Patuxent River, stars represent Kent Island, squares represent the coastal bays, and circles represent inner Chesapeake Bay. At $\Delta K = 2$, the Patuxent River forms a cluster while the remaining sampling localities form a second cluster. This second cluster is composed of three subclusters ($\Delta K = 3$), which contains Kent Island, inner Chesapeake Bay, and the coastal bays.

transponder tags to prevent resampling. Blood samples were preserved on FTA cards (Whatman, Inc., Clifton, NJ, USA). DNA was isolated using Puregene DNA extraction kits (Qiagen, Venlo, Netherlands) and resuspended in TE buffer (10 mM Tris-HCl, pH 8.0, 1 mM EDTA).

We assayed individuals at 12 microsatellite loci (Appendix S2, Supporting Information) developed for the bog turtle (*Glyptemys muhlenbergii*), which amplify in other Emydid turtles (King & Julian 2004). Each PCR consisted of 100–200 ng of genomic DNA, 0.88 μL PCR buffer (59 mM Tris-HCl, pH 8.3; 15 mM $(NH_4)_2SO_4$; 9 mM ß-mercaptoethanol; 6 mM EDTA), 3.75 mM $MgCl_2$, 0.31 mM dNTPs, 0.15–0.25 mM of forward and reverse primers, and 0.4 U AmpliTaq. All samples were brought up to a total volume of 20 μL with deionized water. Each forward primer was 5′ modified with FAM, NED or HEX fluorescent labels (Applied Biosystems, Waltham, MA, USA). The following amplification conditions were used: 94 °C for 2 min; 35 cycles of 94 °C denaturation for 45 s, 56 °C annealing for 45 s, 72 °C extension for 2 min; final extension of 72 °C for 10 min. Thermal cycling was performed in an MJ DNA Engine PTC 200 (MJ Research, Watertown, MA, USA).

Fragment analysis and allelic designations followed King *et al.* (2006). Capillary electrophoresis was conducted on an ABI Prism 3100 Genetic Analyzer using GeneScan-500 ROX size standard (Thermo Fisher Scientific – Applied Biosystems, Waltham, MA, USA). Fragment size data were generated using GENESCAN software version 3.7 (Applied Biosystems). GENOTYPER software version 3.6 (Applied Biosystems) was used to score, bin and assign genotypes for each individual. We used MICRO-CHECKER version 2.2.3 (Oosterhout *et al.* 2004), including 10 000 Monte Carlo simulations to test for the presence of null alleles and estimate 95% confidence intervals. No evidence of null alleles was detected at any locus.

Population structure and genetic diversity

We used STRUCTURE version 2.3 (Pritchard *et al.* 2000) to infer the number of genotypic clusters in the Chesapeake Bay region. STRUCTURE identifies populations by maximizing conformity to Hardy–Weinberg equilibrium (HWE) while simultaneously minimizing linkage disequilibrium within K user-defined clusters. We ran STRUCTURE from $K = 1$ to $K = 15$ populations, with each value of K run ten times with randomly generated starting seeds. Each Markov Chain Monte Carlo (MCMC) run consisted of 550 000 iterations, with the first 250 000 discarded as burn-in. We used the admixture model, the correlated allele frequencies prior, the LOCprior, the LOCISPOP prior, fixed λ and inferred α. We used sampling localities (Fig. 1) as priors for the LOCprior. STRUCTURE results were collated and ΔK computed via the Evanno method (Evanno *et al.* 2005) using STRUCTURE HARVESTER web version 0.6.94 (Earl &

vonHoldt 2011). Label switching and multimodality on preferred values of ΔK were addressed using CLUMPP version 1.1.2 (Jakobsson & Rosenberg 2007), and the final results were visualized using DISTRUCT version 1.1 (Rosenberg 2003). We repeated this procedure within STRUCTURE clusters to detect substructure. We also partitioned genetic variance using an analysis of molecular variance (AMOVAS) in the software ARLEQUIN version 3.5.1.3 (Excoffier & Lischer 2010). Populations were partitioned by landscape features (river, bay and coast), sampling locality and STRUCTURE clusters. Significance was assessed using 1000 permutations. We further estimated population differentiation by quantifying D_{est} (Jost 2008) in the R package DEMETICS version 0.8-7 (Gerlach *et al.* 2010) between all STRUCTURE clusters. We determined significance and estimated 95% confidence intervals using 1000 bootstrap replicates and Bonferroni correction (Dunn 1961). We used FSTAT version 2.9.3 (Goudet 1995) to estimate allelic richness, allele count and linkage disequilibrium for all sampling localities, and ARLEQUIN to estimate heterozygosity and deviations from HWE.

Mutation rate

Because coalescent estimates of historical gene flow and effective population sizes are scaled by mutation rate, we estimated a mutation rate (μ) using approximate Bayesian computation (ABC) in POPABC version 1.0 (Lopes *et al.* 2009). Mutations were modelled using the stepwise-mutation model (SMM; Kimura & Ohta 1978) and were measured in mutations^{-1} site^{-1} generation^{-1}. Demographic parameters were estimated under the isolation–migration model (Nielsen & Wakeley 2001; Hey & Nielsen 2004). Priors for this analysis are summarized in Table 1. We modelled our mutation rate hyperprior using a log-normal distribution centred at 1×10^{-3} (SD = 0.5; Hedrick 1996; Whittaker *et al.* 2003). Genetic tree topology was modelled under a uniform prior. We simulated 2 500 000 genetic trees and ran the ABC-rejection algorithm with a tolerance of 0.0004, retaining the 1000 closest simulated points. We did not run an ABC-regression analysis as some of the summary statistics exhibited multicollinearity, violating the assumptions of local linear regression (Beaumont *et al.* 2002). Following the rejection step, we estimated the mode, 2.5% quantile, and 97.5% quantile for μ in R.

Effective population size

We used MIGRATE version 3.6.5 (Beerli 2008) to jointly estimate θ ($=4N_e\mu$) while estimating M (see below) and used the mutation rate estimated by POPABC to convert θ into N_e. We also estimated effective population sizes using ONESAMP v. 1.2 (Tallmon *et al.* 2008), which uses ABC and eight common summary statistics (e.g. observed heterozygosity, Wright's F_{IS}) to estimate N_e for a single population (Tallmon *et al.* 2008). For these analyses, we ran each STRUCTURE population individually and set lower and upper boundaries for N_e to 2 and 1000, respectively.

Historical gene flow

We used MIGRATE to estimate gene flow levels in Chesapeake Bay prior to European colonization (historical gene flow, M: proportion of migrants per generation, scaled by mutation rate). Because MIGRATE operates in a coalescent framework, it estimates gene flow over long periods of time, up to ~$4N_e$ generations (thousands of years) for larger populations (Beerli 2009). We used populations demarcated by STRUCTURE as a priori population assignments in MIGRATE. To improve speed, we used a Brownian motion model to approximate a stepwise-mutation model. Using slice sampling, we ran four statically heated parallel chains (heated at 1.0, 1.5, 3.0 and 1 000 000) for 30 000 000 iterations, sampled every 3000 iterations, and excluded 7 500 000 iterations as burn-in. MCMC estimates of M were modelled with a uniform prior containing lower and upper boundaries of 0 and 2000. F_{ST} values were used for initial estimates of M. A full migration model was used, which facilitates comparisons with geneflow estimates made in BAYESASS. We considered parameter estimates accurate if an effective sample size (ESS) of 1000 or greater was observed (P. Beerli, personal communication)

Contemporary gene flow

Contemporary rates of gene flow (m: proportion of migrants per generation) in Chesapeake Bay were estimated using BAYESASS version 3.0 (Wilson & Rannala 2003). BAYESASS estimates all pairwise migration rates among populations. According to Wilson & Rannala (2003), BAYESASS estimates gene flow '…over the last several generations.' Following Chiucchi & Gibbs (2010), we assumed this to mean roughly five generations. Using a generation time of 12 years (W. Roosenburg, unpublished data), BAYESASS is quantifying gene flow within the last 60 years or so, a time period characterized by extensive anthropogenic influences, including habitat loss and fragmentation. We used populations demarcated by STRUCTURE as a priori population assignments. We ran 10 MCMC simulations (Faubet *et al.* 2007) with different starting seeds for 20 000 000 iterations, sampling every 2000 iterations; 10 000 000 iterations were excluded as burn-in. Chain mixing delta parameters were adjusted in pilot runs to

Table 1 Summary of the parameters and priors used in popABC. 2 500 000 genetic trees were simulated and a tolerance of 0.0004 was applied, resulting in 1000 simulated data points. ICB = inner Chesapeake Bay, Patuxent = Patuxent River, Kent = Kent Island and CoB = coastal bays

Parameter	Description	Prior
μ	Mutation Rate (site^{-1} generation^{-1})	Lognormal (−3.0,0.5,0.5,0.5)
N_e1	Effective Population Size, Kent Island (individuals)	Uniform (0, 5000)
N_e2	Effective Population Size, Patuxent (individuals)	Uniform (0, 5000)
N_e3	Effective Population Size, ICB (individuals)	Uniform (0, 5000)
N_e4	Effective Population Size, CoB (individuals)	Uniform (0, 5000)
N_eA1	Ancestral Population Size (individuals)	Uniform (0, 10 000)
N_eA2	Ancestral Population Size (individuals)	Uniform (0, 10 000)
N_eA3	Ancestral Population Size (individuals)	Uniform (0, 10 000)
m1	Kent -> Patuxent Migration Rate (fraction of immigrants)	Uniform (0, 0.1)
m2	Patuxent -> Kent Migration Rate (fraction of immigrants)	Uniform (0, 0.1)
m3	ICB -> CoB Migration Rate (fraction of immigrants)	Uniform (0, 0.1)
m4	CoB -> ICB Migration Rate (fraction of immigrants)	Uniform (0, 0.1)
m_A1	Ancestral Migration Rate (fraction of immigrants)	Uniform (0, 0.1)
m_A2	Ancestral Migration Rate (fraction of immigrants)	Uniform (0, 0.1)
$T_{ev}1$	Splitting Event 1 (years)	Uniform (0, 5000)
$T_{ev}2$	Splitting Event 2 (years)	$T_{ev}1$ + Uniform (0, 5000)
$T_{ev}3$	Splitting Event 3 (years)	$T_{ev}2$ + Uniform (0, 5000)
τ	Generation Time	12 years (constant)
Top	Tree Topology (18 possible arrangements)	Uniform (0, 18)

maintain a MCMC state-change acceptance ratio of 20–40%, the empirically recommended window (Rannala 2011). We diagnosed MCMC stationarity for each run in TRACER version 1.5. (Rambaut & Drummond 2007) and used a Bayesian deviancy measure (Spiegelhalter *et al.* 2002) to determine which run best fit the data with R (Meirmans 2014). We took the starting seed from this best-fit run and ran a MCMC for 50 000 000 iterations, sampled every 2000 iterations, with the first 20 000 000 iterations excluded as burn-in. We visualized MCMC stationarity for this final run in TRACER. The ESS for all parameters was >200.

Comparison of historical and contemporary gene flow

We tested for a relationship between historical and contemporary gene flow by conducting a Mantel test in the R package VEGAN version 2.2-1 (Oksanen *et al.* 2013) using 100 000 permutations. To compare historical estimates of gene flow generated by MIGRATE ($M = m_h/\mu$) to contemporary estimates of gene flow from BAYESASS, we multiplied the M-values generated by MIGRATE by the mutation rate estimated in POPABC. We then subtracted these values from the contemporary estimates of gene flow from BAYESASS ($\Delta m = m - m_h$). The resulting value, Δm, denotes temporal changes in gene flow. Negative values of Δm indicate reduced gene flow in the present, positive values indicate increased gene flow, and values near zero indicate no change.

Population bottlenecks

Because estimates of θ and M are sensitive to fluctuations in effective population size (Beerli 2009), we conducted tests to detect bottlenecks. We tested for bottlenecks at two generational time scales. First, we tested for bottlenecks using a mode-shift test, which is capable of detecting bottlenecks '…within the past few dozen generations,' (Luikart & Cornuet 1998). Older bottlenecks were tested for using a Wilcoxon's sign-rank test, which detects bottlenecks 25–250 generations in the past (Cornuet & Luikart 1996). Bottleneck tests were conducted in the program BOTTLENECK version 1.2.02 (Piry *et al.* 1999). We ran BOTTLENECK under the SMM and the two-phase model (TPM) and tested for heterozygosity excess. Under the TPM, we set 95% of all mutations to be single-step with 12% variance within multistep mutations, following the recommendation of Piry *et al.* (1999). All tests were conducted using 50 000 permutations and analysed by STRUCTURE cluster. Because small sample sizes can lead to low statistical power in detecting bottlenecks (Peery *et al.* 2012), we also pooled all samples together and reran all tests for the entire Chesapeake Bay region ($n = 617$).

Results

Population structure and genetic diversity

Measures of genetic diversity showed high levels of heterozygosity, allelic richness and allele counts for

sampling localities relative to other regions (Hauswaldt & Glenn 2005; Hart *et al*. 2014; Appendix S3, Supporting Information). Sampling localities had mean expected and observed heterozygosities between 0.69 and 0.78, a mean of 6–8 alleles per locus and mean allelic richness between 5.8 and 6.5. No loci were found to be in linkage disequilibrium. Across all populations and loci, 7 of 165 loci were out of HWE at $\alpha = 0.05$, but only one locus in one population (MD1) was out of HWE after Bonferroni correction (Appendices S3 and S4, Supporting Information).

Preliminary runs of STRUCTURE did not detect genetic structure within Chesapeake Bay. This was because locus D21 was nearly monomorphic. Removing this locus ameliorated the problem, and all results presented have locus D21 removed. In total, we identified four terrapin populations (Fig. 1): the Patuxent River, Kent Island, the coastal bays and inner Chesapeake Bay. Initial runs of STRUCTURE found the Patuxent River (MD3, MD4) to form the first cluster (Appendix S5, Supporting Information), with the remaining localities forming a second cluster (Fig. 1, $\Delta K = 2$). Analysis of the second cluster (Fig. 1, $\Delta K = 3$) revealed it was composed of three subclusters (Appendix S5, Supporting Information): Kent Island (MD2, MD8), the coastal bays (VA2, VA3, VA4) and inner Chesapeake Bay (MD1,5,6,7,9,10,11, VA1).

AMOVAs indicated that most of the genetic variance in Chesapeake Bay is found within populations (Appendix S6, Supporting Information). STRUCTURE clusters explained the most genetic variation (0.96% $P = 0.0031$), while landscape features (0.88% $P = 0.0154$) and sampling locality (0.88% $P < 0.001$) explained slightly less. Estimates of D_{est} among STRUCTURE clusters identified significant levels of population differentiation among all clusters (Table 2). Kent Island and inner Chesapeake Bay were estimated to be the most similar ($D_{est} = 0.0155$), while the Patuxent River and the coastal bays were estimated to be the most dissimilar ($D_{est} = 0.0654$).

Mutation rate

ABC posterior estimates of μ solved at a mode of 4.3×10^{-4} mutations^{-1} site^{-1} generation^{-1} (Fig. 2). This estimate of μ is similar to a commonly assumed microsatellite mutation rate of 5.0×10^{-4} (e.g. Estoup *et al*. 2002; Faubet *et al*. 2007; Chiucchi & Gibbs 2010).

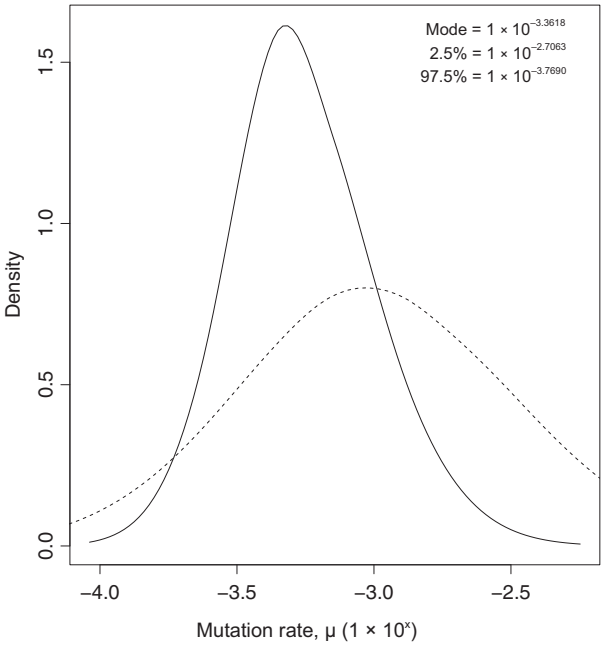

Fig. 2 Approximate Bayesian computation posterior (solid line) and hyperprior (dotted line; log-normal) distributions for μ, the mutation rate used to convert θ into N_e and M into m_h (MIGRATE), for comparisons with m from BAYESASS. The mode is $1 \times 10^{-3.36}$, or 4.3×10^{-4} mutations^{-1} site^{-1} generation^{-1}.

Effective population size

Estimates of N_e from MIGRATE produced a range of effective population sizes in Chesapeake Bay (Fig. 3A). Inner Chesapeake Bay was estimated to have the largest effective population size, at $N_e = 758$ (95% CI: 476–1398). The Patuxent River was the next largest, at $N_e = 144$ (8–261), followed by Kent Island, at $N_e = 109$ (19–261), and the coastal bays, at $N_e = 98$ (0–238). ONESAMP generated the same order of population sizes, but differed in its estimates. Inner Chesapeake Bay was estimated to have an effective size of 302 (265–361), the Patuxent River = 254 (195–467), Kent Island = 154 (139–188) and the coastal bays = 100 (78–158).

Table 2 Estimates of population differentiation. Values below the diagonal are D_{est} values, with 95% CIs in brackets. Values above the diagonal represent *P*-values, with Bonferroni corrections shown in parentheses

	Kent Island	Patuxent River	Coastal Bays	Inner CB
Kent Island	—	0.001 (0.006)	0.001 (0.006)	0.001 (0.006)
Patuxent River	0.0443 [0.0380–0.0523]	—	0.001 (0.006)	0.001 (0.006)
Coastal Bays	0.0374 [0.0320–0.0486]	0.0654 [0.0576–0.0747]	—	0.001 (0.006)
Inner CB	0.0155 [0.0116–0.0219]	0.0291 [0.0254–0.0343]	0.0333 [0.0274–0.0414]	—

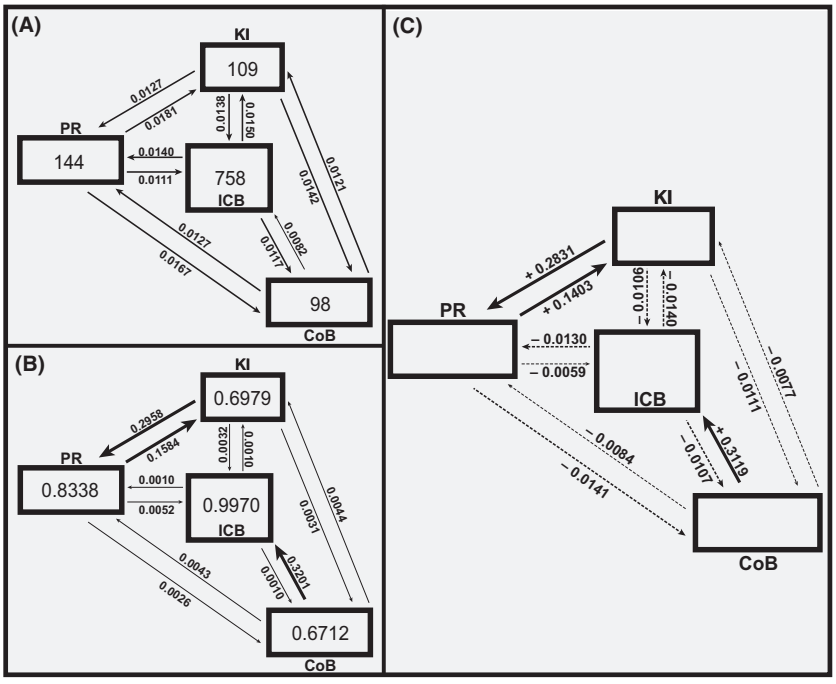

Fig. 3 Gene flow in Chesapeake Bay. KI = Kent Island, PR = the Patuxent River, ICB = inner Chesapeake Bay, and CoB = the coastal bays. Thin lines represent estimates of m or Δm of <0.01, intermediate lines represent estimates of 0.01–0.05, and thick lines represent estimates of >0.05. (A) Results from MIGRATE. Numbers within boxes denote N_e, while values above arrows indicate proportion of immigrants (m_h). (B) Contemporary gene flow rates determined by BAYESASS. Numbers within boxes indicate the proportion of individuals to remain within the population, and values above arrows indicate the proportion of immigrants (m) to their respective populations. (C) Historical gene flow rates subtracted from contemporary rates ($m - m_h = \Delta m$). Dashed arrows indicate gene flow routes that have reduced contemporary gene flow ($-\Delta m$) and solid arrows indicate routes that have increased contemporary gene flow ($+\Delta m$).

Historical gene flow

Estimates of historical geneflow rates revealed similar but low levels of gene flow among all populations (Fig. 3A). Historical geneflow levels from the coastal bays to inner Chesapeake Bay were the lowest of all routes ($m = 0.0082$), while levels of gene flow from the Patuxent River to Kent Island were the highest ($m = 0.0181$).

Contemporary gene flow

Contemporary levels of gene flow in Chesapeake Bay showed much more variation than did historical levels (Fig. 3B). Gene flow leaving inner Chesapeake Bay was the lowest of all contemporary levels ($m = 0.0010$), while gene flow emigrating from the coastal bays into inner Chesapeake Bay was the highest ($m = 0.3201$). Gene flow between Kent Island and the Patuxent River was also markedly higher than gene flow between other populations ($m = 0.2958$ and $m = 0.1584$, respectively). Of the six paired geneflow routes, only two were found to be asymmetrical (nonoverlapping 95% CI): gene flow between Kent Island and the Patuxent River, and gene flow between the coastal bays to inner Chesapeake Bay.

Comparison of historical and contemporary gene flow

A Mantel test did not detect a relationship between historical and contemporary gene flow ($r = 0.86$, $P = 0.16667$). Three rates were found to increase substantially through time (Fig. 3C, solid lines). Contemporary geneflow levels from Kent Island to the Patuxent River and gene flow from the Patuxent River to Kent Island were much higher than historical levels ($\Delta m = +0.2831$ and $\Delta m = +0.1403$, respectively), as were geneflow levels from the coastal bays to inner Chesapeake Bay ($\Delta m = +0.3119$). We removed these routes and performed another Mantel test, but found no significant relationship ($r = 0.86$, $P = 0.125$), as all other routes showed varying degrees of geneflow reduction, approximately $\Delta m \approx -0.01$. The Patuxent River to inner Chesapeake Bay ($\Delta m = -0.0059$) and the coastal bays to the Patuxent River ($\Delta m = -0.0084$) showed the least change in geneflow levels over time.

Population bottlenecks

Bottleneck tests failed to detect any signatures of heterozygosity excess in Chesapeake Bay terrapins (Appendix S7, Supporting Information). Similarly, a mode-shift test failed to detect any bottlenecks, with all populations assuming a normal 'L-shaped' distribution. When the data were pooled to correct for low power associated with small sample sizes (Peery *et al.* 2012), the same results were recovered (Appendix S7, Supporting Information).

Discussion

Given the extent of habitat fragmentation and its contribution to the ongoing biodiversity crisis, conservation

efforts are often aimed at evaluating and ameliorating levels of connectivity between populations (Wilcox & Murphy 1985; Hanski & Gilpin 1997; Beier *et al.* 2008; Newmark 2008). Many such studies assume that population connectivity was higher prior to anthropogenic changes, but this is not always the case, and there is commonly a disconnect between ecological estimates of dispersal and levels of genetic fragmentation (Kuchta & Tan 2006; Epps *et al.* 2013).

We delineated four terrapin populations in the Chesapeake Bay region that exhibited high levels of heterozygosity and allelic diversity (Fig. 1; Appendix 3, Supplementary Information) and weak structure (Fig. 1; Appendix S6, Supporting Information). Historical estimates of migration indicate that gene flow was limited among all populations ($m_h \approx 0.01$; Fig. 3A). By contrast, contemporary estimates of migration were more variable (Fig. 3B). While most populations remained connected by low levels of gene flow, substantial increases in gene flow were detected between Kent Island and the Patuxent River ($\Delta m = +0.2831$ and $\Delta m = +0.1403$) and from the coastal bays into inner Chesapeake Bay ($\Delta m = +0.3119$; Fig. 3C).

The documented increases in contemporary gene flow may have been human-mediated, as terrapins are known to have been translocated into and around Chesapeake Bay to supplement terrapin farms. Terrapins were first brought into Chesapeake Bay from North Carolina around 1909, and were reportedly released when the terrapin farms closed (Hildebrand & Hatsel 1926; Hildebrand 1933). This transport of terrapins could explain our substantial increase in gene flow from the coastal bays to inner Chesapeake Bay ($\Delta m = +0.3119$; Fig. 3C). Alternatively, the increase in gene flow could be due to natural processes. Hauswaldt & Glenn (2005) demonstrated that 75% of Chesapeake Bay terrapins could be correctly assigned to their population of origin using only six microsatellite loci and that Chesapeake Bay populations have higher numbers of private alleles than neighbouring populations. If translocations from North Carolina represented a large influx of genetic variation, one might expect assignment tests to confound Chesapeake Bay terrapins with terrapins from North Carolina, which was not the case. Increased spatial sampling is needed to determine whether our documented increase in contemporary gene flow into Chesapeake Bay is due to the natural movement of individuals or is due to translocation from North Carolina or another source.

The Patuxent River and Kent Island also exhibited large temporal increases in gene flow between them (Fig. 3C). This too may be caused by translocation, as the largest terrapin farm in Chesapeake Bay was located on the Patuxent River at one time, and reportedly '...consist[ed] of a large salt water lake, which could accommodate thousands of terrapins...' (Carpenter 1891). So far as we know, this farm was stocked prior to imports of terrapins from North Carolina, and thus, the terrapins farmed on the Patuxent River were most likely from Chesapeake Bay. Populations located near Kent Island and the Patuxent River represent nearby sources for the farm. Thus, anthropogenic translocation could be the cause of the detected contemporary increases in gene flow. Alternatively, it is possible that the increases in contemporary gene flow are the product of natural increases in genetic connectivity, despite the high levels of habitat fragmentation in the region. Relative to the eastern shoreline, the western shore of Chesapeake Bay lacks jutting peninsulas (Fig. 1). This lack of peninsulas may act as a conduit of gene flow between Kent Island and the Patuxent River, as movement between these populations is not as circuitous as dispersal along the eastern shore. However, this requires dispersal distances that are not commonly documented in ecological studies.

In contrast to the increases in contemporary gene flow discussed above, the majority of populations exhibited decreased contemporary gene flow. Within Chesapeake Bay, substantial habitat modification has occurred within the last century. In particular, shorelines have become reinforced with riprap to prevent erosion. Female terrapins prefer to nest on sandy beaches (Roosenburg 1994) and usually return to the same location each nesting season (Szerlag & McRobert 2006). Moreover, studies show that offspring exhibit natal philopatry (Sheridan *et al.* 2010). As sandy beaches are lost to shoreline development, females are restricted to fewer nesting locations, increasing population fragmentation. In addition, even where terrapins can nest, the mortality risk for eggs, hatchlings and adult females has increased, as raccoons (*Procyon lotor*) and other mesopredators thrive in human-modified landscapes (Crooks & Soulé 1999). Some nesting locations suffer mortality rates as high as 92% for nests (Feinberg & Burke 2003) and 10% for adult females (Siegel 1980).

While gravid females face higher mortality during terrestrial nesting excursions, juvenile females and males of all age classes experience increased mortality in aquatic habitats as fisheries bycatch. Crab pots are used to harvest Blue Crabs (*Callinectes sapidus*), and males and juvenile females (both of which are smaller than adult females) commonly become entrapped in crab pots and drown (Roosenburg *et al.* 1997; Roosenburg & Green 2000). While several states now require a bycatch reduction device (BRD) to exclude terrapins, Maryland only requires them in recreational crab pots. However, BRD compliance for recreational crab pots in Maryland is under 35% (Radzio *et al.* 2013). Terrapins

are characterized by male-biased dispersal (Sheridan *et al.* 2010), and thus, males in particular experience an increased risk of mortality due to fishery activities. We suggest that the increased mortality risk of dispersing males has lowered contemporary geneflow rates among populations.

While it is well documented that terrapins underwent population contractions due to overharvesting and other factors (Garber 1988; Garber 1990), we failed to find evidence of a population bottleneck in Chesapeake Bay. This surprising result may be a consequence of translocation, which would have subsidized populations by re-introducing genetic diversity, and may have confounded efforts to detect a genetic bottleneck (Hauswaldt & Glenn 2005; this study). Indeed, natural populations can be greatly effected by translocation, with potential benefits (Westemeier *et al.* 1998) or unforeseen consequences (Frankham *et al.* 2002). More work on bottleneck detection using genetic data is badly needed as bottleneck tests using heterozygosity excess may fail to detect bottlenecks in populations known to have experienced substantial declines (Funk *et al.* 2010; Peery *et al.* 2012).

The Diamondback Terrapin has been the focus of much conservation attention, and a number of ecological studies indicate that terrapins generally exhibit limited dispersal and high levels of philopatry, which over time would lead to the build-up of genetic structure (Butler 2002; Converse & Kuchta *in press*; Gibbons *et al.* 2001; Roosenburg 1994; Sheridan *et al.* 2010; Spivey 1998). By contrast, genetic studies find that terrapin populations are weakly differentiated, even at regional scales (Drabeck *et al.* 2014; Sheridan *et al.* 2010; Hauswaldt & Glenn 2005; Hart *et al.* 2014; Petre 2014). One hypothesis to reconcile these data is that terrapins migrate large distances (several kilometres) to mating aggregations, which would prevent the build-up of genetic structure among populations (Hauswaldt & Glenn 2005). However, work by Sheridan (2010) suggests that terrapins do not travel long distances to mating aggregations. We propose a modification to Hauswaldt & Glenn's (2005) hypothesis: that mating behaviour and population sex ratios jointly function to limit genetic structure. Under this hypothesis, terrapins form mating aggregations near their home ranges, which homogenizes populations at the local level. Similarly, dispersal by male terrapins promotes admixture among mating aggregations. Male-biased dispersal has large genetic consequences because populations in Chesapeake Bay exhibit highly unequal sex ratios. For example, at Poplar Island and the Patuxent River, female terrapins outnumber males nine to one (9:1) and three to one (3:1), respectively (W. Roosenburg, unpublished data). Biased sex ratios allow dispersing males to disproportionately contribute their genetic material to host populations. Furthermore, female terrapins mate multiple times, store sperm and lay clutches of mixed paternity (Hauswaldt 2004; Sheridan 2010), increasing the odds of mating with immigrant males. It also remains possible that ecological studies document structure that is genetically nascent (Landguth *et al.* 2010).

Our results have important implications for the management of species in heavily modified landscapes. Anthropogenic habitat fragmentation is an ongoing contributor to the biodiversity crisis, and the study of metapopulation connectivity is crucial for setting appropriate conservation targets (Wilcox & Murphy 1985). However, current population genetic structure is the product of the joint influence of contemporary and historical processes, and thus, to assess contemporary changes in connectivity, it is necessary to consider the historical context. Contrary to our initial hypothesis of substantial decreases in contemporary gene flow among terrapin populations as a consequence of habitat loss and fragmentation, we documented enormous increases in gene flow into Chesapeake Bay and between two populations within Chesapeake Bay. We hypothesize that this is due to translocation events associated with terrapin farming. Without an estimate of historical levels of connectivity, however, it would not have been clear that the high contemporary geneflow estimates were a recent phenomenon; indeed, we may have interpreted the relatively low estimates of contemporary gene flow among most other populations as indicative of reduced dispersal! Incorporating historical processes greatly improves interpretation of contemporary processes (Vandergast *et al.* 2007; Hansen *et al.* 2009; Pavlacky *et al.* 2009; Epps *et al.* 2013; Husemann *et al.* 2015). Our results confirm the importance of taking historical factors into account when quantifying genetic connectivity in highly impacted landscapes.

Acknowledgements

We thank Kristen Hart, Colleen Young, Robin Johnson, Daniel Day and others for sample collection, genotyping and logistical support. We thank the Hooper Lab at Ohio University for allowing access to their computer cluster. We thank Ohio University, the Ohio Center for Ecology and Evolutionary Studies, and the United States Geological Survey for financial and logistical support. We thank the KRW discussion group at Ohio University for input and suggestions. We thank the five anonymous reviewers who greatly improved the quality of the manuscript. We thank Tracey Saxby, Kate Boicourt, and the Integration and Application Network, University of Maryland Center, for Environmental Science for high-resolution images of Chesapeake Bay. Use of trade, product or firm names does not imply endorsement by the United States government.

References

Auger PJ (1989) Sex ratio and nesting behavior in a population of *Malaclemys terrapin* displaying temperature-dependent sex-determination. Ph.D. dissertation, Tufts University, Medford, MA, 174 pp.

Banks SC, Cary GJ, Smith AL *et al.* (2013) How does ecological disturbance influence genetic diversity? *Trends in Ecology and Evolution*, **28**, 670–679.

Barney RL (1924) Further notes on the natural history and artificial propagation of the diamond-back terrapin. *Bulletin of the US Bureau of Fisheries*, **38**, 91–111.

Barr KR, Kus BE, Preston KL, Howell S, Perkins E, Vandergast AG (2015) Habitat fragmentation in coastal southern California disrupts genetic connectivity in the cactus wren (*Campylorhynchus brunneicapillus*). *Molecular Ecology*, **24**, 2349–2363.

Beaumont MA, Zhang W, Balding DJ (2002) Approximate Bayesian computation in population genetics. *Genetics*, **162**, 2025–2035.

Beerli P (2008) Migrate version 3.6.5: a maximum likelihood and Bayesian estimator of gene flow using the coalescent. Distributed over the internet at http://popgen.scs.edu/migrate.html.

Beerli P (2009) How to use MIGRATE or why are Markov chain Monte Carlo programs difficult to use. In: *Population Genetics for Animal Conservation* (eds Bertorell G, Bruford MW, Hauffe HC, Rizzoli A, Vernesi C), pp. 42–79. Cambridge University Press, Cambridge.

Beier P, Majka DR, Spencer WD (2008) Forks in the road: choices in procedures for designing wildlife linkages. *Conservation Biology*, **22**, 836–837.

Bowler DE, Benton TG (2005) Causes and consequences of animal dispersal strategies: relating individual behaviour to spatial dynamics. *Biological Reviews of the Cambridge Philosophical Society*, **80**, 205–225.

Braunisch V, Segelbacher G, Hirzel AH (2010) Modeling functional landscape connectivity from genetic population structure: a new spatially explicit approach. *Molecular Ecology*, **19**, 3664–3678.

Butler JA (2002) Population ecology, home range, and seasonal movements of the Carolina diamondback terrapin, *Malaclemys terrapin centrata* in northeastern Florida. Florida Fish and Wildlife Conservation Commission, Tallahassee, FL, 72 pp.

Caizergues A, Bernard-Laurent A, Brenot JF, Ellison L, Rasplus JY (2003) Population genetic structure of rock ptarmigan *Lagopus mutus* in Northern and Western Europe. *Molecular Ecology*, **12**, 2267–2274.

Callens T, Galbusra P, Matthysen E *et al.* (2011) Genetic signature of population fragmentation varies with mobility in seven bird species of a fragmented Kenyan cloud forest. *Molecular Ecology*, **20**, 1829–1844.

Carpenter FG (1891) An age of Terrapin. In: *Current Literature: A Magazine of Record and Review*, **vol. VI** (ed Somers F), pp. 246–247. The Current Literature Publishing Company, New York.

Castillo JA, Epps CW, Davis AR, Cushman SA (2014) Landscape effects on gene flow for a climate-sensitive montane species, the American pika. *Molecular Ecology*, **23**, 843–856.

Cecala KK, Gibbons JW, Dorcas ME (2008) Ecological effects of major injuries in diamondback terrapins: implications for conservation and management. *Aquatic Conservation: Marine and Freshwater Ecosystems*, **19**, 421–427.

Chiucchi JE, Gibbs HL (2010) Similarity of contemporary and historical gene flow among highly fragmented populations of an endangered rattlesnake. *Molecular Ecology*, **19**, 5345–5358.

Coker R (1906) The natural history and cultivation of the diamond-back terrapin with notes on other forms of turtles. *North Carolina Geological Survey Bulletin*, **14**, 1–67.

Coker R (1920) The diamond-back terrapin: past, present, and future. *Scientific Monthly*, **11**, 171–186.

Converse PE, Kuchta SR (in press) Molecular ecology and phylogeography of the Diamond-backed Terrapin. In: *The Ecology and Conservation of Diamond-backed Terrapins, Malaclemys terrapin* (eds Kennedy V, Roosenburg WM). The Johns Hopkins University Press, Baltimore, Maryland.

Cornuet JM, Luikart G (1996) Description and power analysis of two tests for detecting recent population bottlenecks from allele frequency data. *Genetics*, **144**, 2001–2014.

Crispo E, Moore J-S, Lee-Yaw JA, Gray SM, Haller BC (2011) Broken barriers: human-induced changes to gene flow and introgression in animals. *Bioassays*, **33**, 508–518.

Crooks KR, Soulé ME (1999) Mesopredator release and avifaunal extinctions in a fragmented system. *Nature*, **400**, 563–566.

Dorcas ME, Willson JD, Gibbons JW (2007) Crab trapping causes population decline and demographic changes in diamondback terrapins over two decades. *Biological Conservation*, **137**, 334–340.

Drabeck DH, Chatfield MWH, Richards-Zawacki CL (2014) The status of Louisiana's Diamondback Terrapin (*Malaclemys terrapin*) populations in the wake of the Deepwater Horizon oil spill: insights from population genetic and contaminant analyses. *Journal of Herpetology*, **48**, 125–136.

Dunn OJ (1961) Multiple comparisons among means. *Journal of the American Statistical Association*, **56**, 52–64.

Earl DA, vonHoldt BM (2011) STRUCTURE HARVESTER: a website and program for visualizing STRUCTURE output and implementing the Evanno method. *Conservation Genetics Resources*, **4**, 359–361.

Epps CW, Palsbøll PJ, Wehausen WD, Roderick GK, Ramey RR II, McCullough DR (2005) Highways block gene flow and cause a rapid decline in genetic diversity of desert bighorn sheep. *Ecology Letters*, **8**, 1029–1038.

Epps CW, Wasser SK, Keim JL, Mutayoba BM, Brashares JS (2013) Quantifying past and present connectivity illuminates a rapidly changing landscape for the African elephant. *Molecular Ecology*, **22**, 1574–1588.

Ernst CH, Barbour RW (1989) *Turtles of the World*. Smithsonian Institution Press, Washington, D.C. and London.

Estoup A, Jarne P, Cornuet J-M (2002) Homoplasy and mutation model at microsatellite loci and their consequences for population genetics analysis. *Molecular Ecology*, **11**, 1591–1604.

Evanno G, Regnaut S, Goudet J (2005) Detecting the number of clusters of individuals using the software structure: a simulation study. *Molecular Ecology*, **14**, 2611–2620.

Excoffier L, Lischer HEL (2010) Arlequin suite ver 3.5: a new series of programs to perform population genetics analyses under Linux and Windows. *Molecular Ecology Resources*, **10**, 564–567.

Faubet P, Waples RS, Gaggiotti OE (2007) Evaluating the performance of a multilocus Bayesian method for the estimation of migration rates. *Molecular Ecology*, **16**, 1149–1166.

Feinberg JA, Burke RL (2003) Nesting ecology and predation of Diamondback Terrapins, *Malaclemys terrapin*, at Gateway National Recreation Area, New York. *Journal of Herpetology*, **37**, 517–526.

Frankham R, Ballou JD, Briscoe DA (2002) *Introduction to Conservation Genetics*. Cambridge University Press, Cambridge.

Funk WC, Forsman ED, Johnson M, Mullins TD, Haig SM (2010) Evidence for recent population bottlenecks in northern spotted owls (*Strix occidentals caurina*). *Conservation Genetics*, **11**, 1013–1021.

Garber SW (1988) Diamondback terrapin exploitation. *Plastron Papers*, **17**, 18–22.

Garber SW (1990) The ups and downs of the diamondback terrapin. *The New York Conservationists*, **44**, 44–48.

Gerlach G, Jueterbock A, Kraemer P, Deppermann J, Harmand P (2010) Calculations of population differentiation based on G_{ST} and D: forget G_{ST} but not all statistics!. *Molecular Ecology*, **19**, 3845–3852.

Gibbons JW, Lovich JE, Tucker AD, FitzSimmons NN, Greene JL (2001) Demographic and ecological factors affecting conservation and management of the Diamondback Terrapin (*Malaclemys terrapin*) in South Carolina. *Chelonian Conservation and Biology*, **4**, 66–74.

Glenos SM (2013) A comparative assessment of diamondback terrapin (*Malaclemys terrapin*) in Galveston Bay, Texas in relation to other northern Gulf Coast populations. Masters thesis, The University of Houston-Clear Lake, TX, 71 pp.

Goudet J (1995) FSTAT (Version 1.2) A computer program to calculate F-statistics. *Journal of Heredity*, **86**, 485–486.

Grosse AM, Dijk JD, Holcomb KL, Maerz JC (2009) Diamondback terrapin mortality in crab pots in a Georgia tidal marsh. *Chelonian Conservation and Biology*, **8**, 98–100.

Gu W, Heikkilä R, Hanski I (2002) Estimating the consequences of habitat fragmentation on extinction risk in dynamic landscapes. *Landscape Ecology*, **17**, 699–710.

Hansen BD, Harley KP, Lindenmayer DB, Taylor AC (2009) Population genetic analysis reveals a long-term decline of a threatened endemic Australian marsupial. *Molecular Ecology*, **18**, 3346–3362.

Hanski IH, Gilpin M (1997) *Metapopulation Biology: Ecology, Genetics, and Evolution*. Academic Press, San Diego, California.

Haramis GM, Henry PF, Day DD (2011) Using scrape fishing to document terrapins in hibernacula in Chesapeake Bay. *Herpetological Review*, **42**, 170–177.

Hart KM, Hunter ME, King TL (2014) Regional differentiation among populations of the Diamondback terrapin (*Malaclemys terrapin*). *Conservation Genetics*, **15**, 593–603.

Hauswaldt JS (2004) Population genetics and mating pattern of diamondback terrapin (*Malaclemys terrapin*). Ph.D. dissertation, University of South Carolina, Columbia, SC, 216 pp.

Hauswaldt JS, Glenn TC (2005) Population genetics of the diamondback terrapin (*Malaclemys terrapin*). *Molecular Ecology*, **14**, 723–732.

Hay WP (1917) Artificial propagation of the diamond-back terrapin. *Bulletin of the US Bureau of Fisheries*, **24**, 1–20.

Hedrick PW (1996) Bottlenecks(s) or metapopulation in cheetas. *Conservation Biology*, **10**, 897–899.

Hey J, Nielsen R (2004) Multilocus methods for estimating population sizes, migration rates and divergence time, with applications to the divergence of *Drosophila pseudoobscura* and *D. persimilis*. *Genetics*, **167**, 747–760.

Hildebrand SF (1929) Review of experiments on artificial culture of diamondback terrapin. *Bulletin of the US Bureau of Fisheries*, **45**, 25–70.

Hildebrand SF (1933) Hybridizing diamond-backed terrapins. *Journal of Heredity*, **113**, 231–238.

Hildebrand SF, Hatsel C (1926) Diamondback terrapin culture at Beaufort, NC. *US Bureau of Fisheries Economic Circular*, **60**, 1–20.

Husemann M, Cousseau L, Callens T *et al*. (2015) Post-fragmentation population structure in a cooperative breeding Afrotropical cloud forest bird: emergence of a source-sink population network. *Molecular Ecology*, **24**, 1172–1187.

Jakobsson M, Rosenberg NA (2007) CLUMPP: a cluster matching and permutation program for dealing with label switching and multimodality in analysis of population structure. *Bioinformatics*, **23**, 1801–1806.

Jost L (2008) G_{ST} and its relatives do not measure differentiation. *Molecular Ecology*, **18**, 4015–4026.

Kimura M, Ohta T (1978) Stepwise mutation model and distribution of allelic frequencies in a finite population. *Proceedings of the National Academy of Sciences*, **75**, 2868–2872.

King TL, Julian SE (2004) Conservation of microsatellite DNA flanking sequence across 13 Emydid genera assayed with novel bog turtle (*Glyptemys muhlenbergii*) loci. *Conservation Genetics*, **5**, 719–725.

King TL, Switzer JF, Morrison CL *et al*. (2006) Comprehensive genetic analyses reveal evolutionarily distinction of a mouse (*Zapus hudsonius preblei*) proposed for delisting from the U.S. Endangered Species Act. *Molecular Ecology*, **15**, 4331–4359.

Kuchta SR, Tan AM (2006) Limited genetic variation across the range of the red-bellied newt, *Taricha rivularis*. *Journal of Herpetology*, **40**, 561–565.

Lande R (1995) Mutation and conservation. *Conservation Biology*, **9**, 782–791.

Landguth EL, Cushman SA, Schwartz MK, Murphy M, McKelvey KS, Luikart G (2010) Quantifying the lag time to detect barriers in landscape genetics. *Molecular Ecology*, **19**, 4179–4191.

Lopes JS, Balding D, Beaumont MA (2009) PopABC: a program to infer historical demographic parameters. *Bioinformatics*, **25**, 2747–2749.

Lovich JE, Gibbons JW (1990) Age at maturity influences adult sex ratio in the turtle *Malaclemys terrapin*. *Oikos*, **59**, 126–134.

Luikart G, Cornuet JM (1998) Empirical evaluation of a test for identifying recently bottlenecked populations from allele frequency data. *Conservation Biology*, **12**, 228–237.

Meirmans PG (2014) Nonconvergence in Bayesian estimation of migration rates. *Molecular Ecology Resources*, **14**, 726–733.

Mitro MG (2003) Demography and viability analyses of a diamondback terrapin population. *Canadian Journal of Zoology*, **81**, 716–726.

Moritz C (1999) Conservation units and translocations: strategies for conserving evolutionary processes. *Hereditas*, **130**, 217–228.

Newmark WD (2008) Isolation of African protected areas. *Frontier in Ecology and the Environment*, **6**, 321–328.

Nielsen R, Wakeley J (2001) Distinguishing migration from isolation: a Markov chain Monte Carlo approach. *Genetics*, **158**, 885–896.

Oksanen J, Blanchet FG, Kindt R *et al.* (2013) vegan: Community Ecology Package. R package version 2010 http://CRAN.R-project.org/package=vegan.

Oosterhout CV, Hutchinson WF, Wills DPM, Shipley P (2004) MICRO-CHECKER: software for identifying and correcting genotyping errors in microsatellite data. *Molecular Ecology Notes*, **4**, 535–538.

Pavlacky DC Jr, Goldizen AW, Prentis PJ *et al.* (2009) A landscape genetics approach for quantifying the relative influence of historic and contemporary habitat heterogeneity on the genetic connectivity of a rainforest bird. *Molecular Ecology*, **18**, 2945–2960.

Peery MZ, Kirby R, Reid BN *et al.* (2012) Reliability of genetic bottleneck tests for detecting recent population declines. *Molecular Ecology*, **21**, 3403–3418.

Petre CL (2014) The conservation genetics of two Emydid turtles: *Emydoidea blandingii* and *Malaclemys terrapin*. Masters thesis, The University of Southern Mississippi, Hattiesburg, MS, 62 pp.

Piry S, Luikart G, Cornuet JM (1999) Computer note. BOTTLENECK: a computer program for detecting recent reductions in the effective size using allele frequency data. *Journal of Heredity*, **90**, 502–503.

Pritchard JK, Stephens M, Donnelly P (2000) Inference of population structure using multilocus genotype data. *Genetics*, **155**, 945–959.

Radzio TA, Roosenburg WM (2005) Diamondback terrapin mortality in the American eel pot fishery and evaluation of a bycatch reduction device. *Estuaries and Coasts*, **28**, 620–626.

Radzio TA, Smolinsky JA, Roosenburg WM (2013) Low use of required terrapin bycatch reduction devices in a recreational crab pot fishery. *Herpetological Conservation and Biology*, **8**, 222–227.

Rambaut A, Drummond AJ (2007) Tracer v1.4. Available from: http://beast.bio.ed.ac.ul/Tracer

Rannala B (2011) BayesAss edition 3.0 user's manual.

Roosenburg WM (1991) The diamondback terrapin: population dynamics, habitat requirements, and opportunities for conservation. New perspectives in the Chesapeake system: a research and management partnership. *Chesapeake Research Consortium Publication*, **137**, 227–234.

Roosenburg WM (1994) Nesting habitat requirements of the diamondback terrapin: a geographic comparison. *Wetland Journal*, **6**, 8–11.

Roosenburg WM, Green JP (2000) Impact of a bycatch reduction device on diamondback terrapin and blue crab capture in crab pots. *Ecological Applications*, **10**, 882–889.

Roosenburg WM, Cresko W, Modesitte M, Robbins MB (1997) Diamondback terrapin (*Malaclemys terrapin*) mortality in crab pots. *Conservation Biology*, **11**, 1166–1172.

Roosenburg WM, Cover J, van Dijk PP (2008) Legislative closure of the Maryland terrapin fishery: perspectives on a historical accomplishment. *Turtle and Tortoise Newsletter*, **12**, 27–30.

Rosenberg NA (2003) Distruct: a program for the graphical display of population structure. *Molecular Ecology Notes*, **4**, 137–138.

Sheridan CM (2010) Mating system and dispersal patterns in the diamondback terrapin (*Malaclemys terrapin*). Ph.D. dissertation, Drexel University, Philadelphia, PA, 204 pp.

Sheridan CM, Spotila JR, Bien WF, Avery HW (2010) Sex-biased dispersal and natal philopatry in the diamondback terrapin, *Malaclemys terrapin*. *Molecular Ecology*, **19**, 5497–5510.

Siegel RA (1980) Nesting habits of diamondback terrapins (*Malaclemys terrapin*) on the Atlantic coast of Florida. *Transactions of the Kansas Academy of Sciences*, **83**, 239–246.

Spiegelhalter DJ, Best NG, Carlin BP (2002) Bayesian measures of model complexity and fit. *Journal of the Royal Statistical Society Series B (Methodological)*, **64**, 583–639.

Spivey PB (1998) Home range, habitat selection, and diet of the diamondback terrapin (*Malaclemys terrapin*) in a North Carolina estuary. Masters thesis, The University of Georgia, Athens, GA, 80 pp.

Szerlag S, McRobert SP (2006) Road occurrence and mortality of the northern diamondback terrapin. *Applied Herpetology*, **3**, 27–37.

Tallmon DA, Koyuk A, Luikart GH, Beaumont MA (2008) ONeSAMP: a program to estimate effective population size using approximate Bayesian computation. *Molecular Ecology Resources*, **8**, 299–301.

Templeton AR, Hemmer H, Mace G, Seal US, Shields WM, Woodruff DS (1986) Local adaption, coadaptation, and population boundaries. *Zoo Biology*, **5**, 115–125.

Templeton AR, Robertson RJ, Brisson J, Strasburg J (2001) Disrupting evolutionary processes: the effect of habitat fragmentation on collared lizards in the Missouri Ozarks. *Proceedings of the National Academy of Sciences*, **98**, 5426–5432.

Vandergast AG, Bohonak AJ, Weissman DB *et al.* (2007) Understanding the genetic effects of recent habitat fragmentation in the context of evolutionary history: phylogeography and landscape genetics of a southern California endemic Jerusalem cricket (Orthoptera: Stenopelmatidae: Stenpelmatus). *Molecular Ecology*, **16**, 977–992.

Weeks AR, Sgro CM, Young AG, Frankham R *et al.* (2011) Assessing the benefits and risks of translocations in changing environments: a genetic perspective. *Evolutionary Applications*, **4**, 709–725.

Westemeier RL, Brawn JD, Simpson SA *et al.* (1998) Tracking long-term decline and recovery of an isolated population. *Science*, **282**, 1695–1698.

Whittaker JC, Harbord RM, Boxall N *et al.* (2003) Likelihood-based estimation of microsatellite mutation rates. *Genetics*, **164**, 781–787.

Wilcox BA, Murphy DD (1985) Conservation strategy: the effects of fragmentation on extinction. *American Naturalist*, **125**, 879–887.

Wilson GA, Rannala B (2003) Bayesian inference of recent migration rates using multilocus genotypes. *Genetics*, **163**, 1177–1191.

Wood RC, Herlands R (1997) Turtles and tires: the impact of road kills on northern diamondback terrapin, *Malaclemys terrapin terrapin*, populations on the Cape May peninsula, southern New Jersey. Proceedings: Conservation, Restoration, and Management of Tortoises and Turtles–An International Conference. New York Turtle and Tortoise Society, New York, USA, 46–53.

P.E.C. and S.R.K. designed and conceived the study. W.M.R., P.F.P.H. and G.M.H. collected field samples. T.L.K. supervised and conducted laboratory work and data collection. P.E.C. and S.R.K. analysed the data. P.E.C. and S.R.K. wrote the manuscript.

Data accessibility

Data used for this article (microsatellite data and all program input files) have been deposited in Dryad, doi:10.5061/dryad.nf8gf.

Supporting information

Additional supporting information may be found in the online version of this article.

Appendix S1 Sampling localities and their abbreviations. Sampling took place from 2003–2005.

Appendix S2. Summary of loci amplified for subsequent analyses.

Appendix S3 Observed heterozygosity (H_o), expected heterozygosity (H_e), allelic richness (A_R), and number of alleles (N_A) by locus for population MD1.

Appendix S4 Pairwise tests of linkage disequilibrium for all loci, based on 1000 permutations and an adjusted *P*-value of 0.00090.

Appendix S5 ΔK plot under the Evanno method for the initial run of STRUCTURE finding the Patuxent River as a genotypic cluster.

Appendix S5 ΔK plot under the Evanno method for the second run of STRUCTURE finding KI, ICB, and CoB as populations.

Appendix S6 AMOVA results indicating terrapin populations in Chesapeake Bay are weakly structured.

Appendix S7 *P*-values for bottleneck detection under each model in BOTTLENECK.

Locality	Sample Size	Latitude	Longitude
Herring Bay, MD (MD1)	25	38.754362	-76.550857
Kent Island, MD (MD2)	38	38.936302	-76.363836
Patuxent River, MD (MD3)	63	38.444332	-76.607811
Buzzard's Island, Patuxent River, MD (MD4)	60	38.489969	-76.652694
Sandy Island Cove, Nanticoke River, MD (MD5)	55	38.260110	-75.947966
Back Cove, Smith Island, MD (MD6)	17	38.021666	-75.998875
Janes Island, MD (MD7)	56	38.007513	-75.849861
Marshy Creek, Kent Island, MD (MD8)	64	38.954972	-76.227814
Northeast Cove, Bloodsworth Island, MD (MD9)	43	38.167177	-76.062002
Tylerton, Smith Island, MD (MD10)	64	37.964927	-76.020185
St. Jerome's Creek, MD (MD11)	16	38.134924	-76.347049
Mobjack Bay, VA (VA1)	45	37.325137	-76.350877
Wachapreague, VA (VA2)	38	37.602862	-75.686380
Metompkin Island, VA (VA3)	20	37.752026	-75.546442
Cedar Island, VA (VA4)	13	37.633496	-75.612748

Appendix S1. Sampling localities and their abbreviations. Sampling took place from 2003-2005.

Locus	Repeat Motif	Fragment Size (bp)	Genbank Accession #
A18	$(GT)_{14}$	109 - 123	AF337648
B08	$(TAC)_{10}$	215 - 242	AF517228
B67	$(TAC)_{13}$	144 - 153	AF517232
B91	$(TAC)_{6}$	125 - 137	AF517234
D21	$(ATCT)_{15}$	150 - 158	AF517236
D55	$(ATCT)_{10}$	170 - 218	AF517240
D62	$(ATCT)_{11}$	128 - 172	AF517241
D87	$(ATCT)_{22}$	223 - 287	AF517244
D90	$(ATCT)_{9}$	109 - 145	AF517247
D93	$(ATCT)_{18}$	148 - 184	AF517248
D114	$(ATCT)_{13}$	86 - 130	AF517251
D121	$(ATCT)_{8}$	129 - 181	AF517252

Appendix S2. Summary of loci amplified for subsequent analyses.

MD1

Locus	H_o	H_e	A_R	N_A
B91	0.44737	0.50351	2.000	2
B08	0.97368	0.85333	5.954	7
D93	0.75758*	0.67739	2.735	3
A18	0.92105	0.76140	4.840	5
D87	0.81579	0.85825	7.652	9
B67	0.39474	0.44737	2.000	2
D90	0.86842	0.85263	7.799	9
D55	0.92105	0.86000	8.352	10
D114	0.71053	0.64807	6.936	8
D121	0.94737***	0.87789$^{\Delta}$	9.590	12
D62	0.78947	0.84035	8.384	10
Avg	0.77700	0.74365	6.022	7.0

* 0.05 ** 0.01 ***0.001

Appendix S3. Observed heterozygosity (H_o), expected heterozygosity (H_e), allelic richness (A_R), and number of alleles (N_A) by locus for population MD1. Significant deviations from Hardy-Weinberg equilibrium are denoted with asterisks. Triangles indicate loci deviating from Hardy-Weinberg equilibrium after Bonferroni correction.

MD2

Locus	H_o	H_e	A_R	N_A
B91	0.40625	0.45485	2.000	2
B08	0.76562	0.84990	6.742	7
D93	0.51562	0.57591	5.365	7
A18	0.73438	0.76784	4.895	5
D87	0.81250	0.83095	7.548	9
B67	0.39062	0.38570	2.000	2
D90	0.93750*	0.85753	7.958	9
D55	0.89062	0.88595	8.094	10
D114	0.85938	0.77227	4.736	5
D121	0.85938	0.88189	8.381	11
D62	0.82540	0.83327	6.815	9
Avg	0.72702	0.66025	5.867	6.9

* 0.05 ** 0.01 ***0.001

Appendix S3. Observed heterozygosity (H_o), expected heterozygosity (H_e), allelic richness (A_R), and number of alleles (N_A) by locus for population MD2. Significant deviations from Hardy-Weinberg equilibrium are denoted with asterisks.

MD8

Locus	H_o	H_e	A_R	N_A
B91	0.58730	0.49943	2.187	3
B08	0.82540	0.83175	7.061	8
D93	0.36842	0.37246	3.680	6
A18	0.66667	0.68063	5.425	7
D87	0.90476	0.86133	8.221	12
B67	0.33333	0.38971	2.000	2
D90	0.87302	0.81600	7.535	10
D55	0.82540	0.83975	9.273	11
D114	0.88889	0.82997	7.226	11
D121	0.88889	0.87721	8.925	12
D62	0.79365*	0.79695	6.452	8
Avg	0.72324	0.70865	6.180	8.2

* 0.05 ** 0.01 ***0.001

Appendix S3. Observed heterozygosity (H_o), expected heterozygosity (H_e), allelic richness (A_R), and number of alleles (N_A) by locus for population MD8. Significant deviations from Hardy-Weinberg equilibrium are denoted with asterisks.

MD3

Locus	H_o	H_e	A_R	N_A
B91	0.46667	0.48403	2.000	2
B08	0.80000	0.85630	7.077	8
D93	0.52542	0.42981	2.377	3
A18	0.70000	0.75378	5.585	8
D87	0.78333	0.79496	8.302	14
B67	0.41667	0.45364	2.000	2
D90	0.81667	0.81190	7.092	9
D55	0.83333	0.86765	7.216	10
D114	0.84746	0.83138	7.571	10
D121	0.90000	0.87955	9.099	12
D62	0.71667	0.79174	6.409	8
Avg	0.70966	0.72316	5.884	7.8

* 0.05 ** 0.01 ***0.001

Appendix S3. Observed heterozygosity (H_o), expected heterozygosity (H_e), allelic richness (A_R), and number of alleles (N_A) by locus for population MD3. No loci were found to be out of HWE.

MD4

Locus	H_o	H_e	A_R	N_A
B91	0.50000	0.57308	2.000	2
B08	0.80000	0.79744	7.454	8
D93	0.65000	0.53462	2.752	3
A18	0.85000	0.77179	5.841	7
D87	1.00000	0.90769	7.398	12
B67	0.05263	0.05263	2.000	2
D90	0.84211	0.83926	6.581	8
D55	0.75000	0.83462	8.355	11
D114	0.60000	0.56026	7.565	9
D121	1.00000	0.90128	8.732	11
D62	0.90000	0.79487	6.433	9
Avg	0.72224	0.68796	5.919	7.5

* 0.05 ** 0.01 ***0.001

Appendix S3. Observed heterozygosity (H_o), expected heterozygosity (H_e), allelic richness (A_R), and number of alleles (N_A) by locus for population MD4. No loci were found to be out of HWE.

MD5

Locus	H_o	H_e	A_R	N_A
B91	0.46154	0.51692	2.218	3
B08	0.84615	0.81231	7.289	9
D93	0.50000	0.49275	3.481	6
A18	0.92308	0.76615	4.766	5
D87	0.84615	0.86462	8.345	11
B67	0.23077	0.40923	2.000	2
D90	0.92308	0.74769	7.523	9
D55	0.92308	0.87385	8.488	11
D114	0.69231	0.68308	6.386	8
D121	1.00000	0.92000	9.461	13
D62	0.69231	0.80000	7.702	10
Avg	0.73077	0.71696	6.151	7.9

* 0.05 ** 0.01 ***0.001

Appendix S3. Observed heterozygosity (H_o), expected heterozygosity (H_e), allelic richness (A_R), and number of alleles (N_A) by locus for population MD4. No loci were found to be out of HWE.

MD9

Locus	H_o	H_e	A_R	N_A
B91	0.42105	0.51895	2.279	3
B08	0.89474	0.82877	7.132	8
D93	0.50000	0.50491	4.301	6
A18	0.78947	0.71789	5.055	6
D87	0.81579	0.86772	7.089	8
B67	0.55263	0.46421	2.000	2
D90	0.84211	0.80211	8.182	10
D55	0.81579	0.86456	8.513	11
D114	0.78947	0.73474	7.134	9
D121	0.94737	0.90035	9.869	13
D62	0.76316	0.77158	7.802	11
Avg	0.73923	0.72507	6.305	7.9

* 0.05 ** 0.01 ***0.001

Appendix S3. Observed heterozygosity (H_o), expected heterozygosity (H_e), allelic richness (A_R), and number of alleles (N_A) by locus for population MD9. No loci were found to be out of HWE.

MD6

Locus	H_o	H_e	A_R	N_A
B91	0.44000	0.50694	2.000	2
B08	0.80000	0.82857	7.536	8
D93	0.40000	0.46694	2.980	3
A18	0.48000	0.66449	3.979	4
D87	0.84000	0.84082	8.146	9
B67	0.40000	0.37224	2.000	2
D90	0.80000	0.81714	7.096	8
D55	0.84000	0.85469	10.046	11
D114	0.80000	0.74939	4.625	5
D121	0.92000	0.88816	10.598	12
D62	0.88000	0.86857	7.633	8
Avg	0.69091	0.71436	6.058	6.5

* 0.05 ** 0.01 ***0.001

Appendix S3. Observed heterozygosity (H_o), expected heterozygosity (H_e), allelic richness (A_R), and number of alleles (N_A) by locus for population MD6. No loci were found to be out of HWE.

MD7

Locus	H_o	H_e	A_R	N_A
B91	0.54545	0.49158	2.000	2
B08	0.83636*	0.84570	7.577	9
D93	0.55556	0.55746	3.467	6
A18	0.85455	0.74395	5.425	7
D87	0.80000	0.86305	8.731	13
B67	0.41818	0.46188	2.214	3
D90	0.78182	0.83253	8.184	11
D55	0.89091	0.85455	8.421	10
D114	0.69091	0.73862	6.851	9
D121	0.85185	0.88629	9.497	12
D62	0.88462	0.84037	7.158	9
Avg	0.73729	0.73782	6.320	8.3

* 0.05 ** 0.01 ***0.001

Appendix S3. Observed heterozygosity (H_o), expected heterozygosity (H_e), allelic richness (A_R), and number of alleles (N_A) by locus for population MD7. Significant deviations from Hardy-Weinberg equilibrium are denoted with asterisks.

MD10

Locus	H_o	H_e	A_R	N_A
B91	0.47059	0.42781	2.000	2
B08	0.82353	0.86096	7.437	8
D93	0.41176	0.55793	3.095	5
A18	0.70588	0.65419	5.374	8
D87	0.70588	0.79857	8.972	12
B67	0.47059	0.49911	2.000	2
D90	0.94118	0.82531	7.349	9
D55	0.88235	0.89483	9.174	12
D114	0.58824	0.63815	7.154	10
D121	0.88235	0.90553	9.109	13
D62	0.87500	0.86492	7.315	11
Avg	0.70521	0.72066	6.271	8.4

* 0.05 ** 0.01 ***0.001

Appendix S3. Observed heterozygosity (H_o), expected heterozygosity (H_e), allelic richness (A_R), and number of alleles (N_A) by locus for population MD10. No loci were found to be out of HWE..

MD11

Locus	H_o	H_e	A_R	N_A
B91	0.48214	0.50306	2.000	2
B08	0.89286	0.85698	6.928	7
D93	0.53571	0.49373	3.000	3
A18	0.75000	0.73198	5.690	6
D87	0.92857	0.87130	8.635	10
B67	0.39286	0.46959	2.000	2
D90	0.83929	0.84749	6.883	7
D55	0.87500	0.87950	9.377	10
D114	0.83636	0.75430	6.853	7
D121	0.87500	0.89318	9.168	10
D62	0.81818	0.82969	6.440	7
Avg	0.74782	0.73916	6.089	6.5

* 0.05 ** 0.01 ***0.001

Appendix S3. Observed heterozygosity (H_o), expected heterozygosity (H_e), allelic richness (A_R), and number of alleles (N_A) by locus for population MD11. No loci were found to be out of HWE.

VA1				
Locus	H_o	H_e	A_R	N_A
B91	0.48837	0.51737	2.000	2
B08	0.74419	0.84213	6.733	7
D93	0.51163	0.59590	3.647	5
A18	0.58140*	0.71546	3.972	4
D87	0.81395	0.79754	7.339	9
B67	0.53488	0.41724	2.000	2
D90	0.83721	0.85855	7.220	9
D55	0.86047	0.85445	8.484	11
D114	0.62791	0.72011	7.499	10
D121	0.88372	0.89877	8.172	11
D62	0.74419	0.84761	7.106	9
Avg	0.69345	0.73319	5.834	7.2
* 0.05 ** 0.01 ***0.001				

Appendix S3. Observed heterozygosity (H_o), expected heterozygosity (H_e), allelic richness (A_R), and number of alleles (N_A) by locus for population VA1. Significant deviations from Hardy-Weinberg equilibrium are denoted with asterisks.

VA3

Locus	H_o	H_e	A_R	N_A
B91	0.44444	0.88343	2.943	3
B08	0.81250	0.82862	6.417	7
D93	0.51562	0.53851	2.600	3
A18	0.67188	0.71026	5.487	6
D87	0.88889	0.88190	9.929	11
B67	0.43750	0.42077	1.632	2
D90	0.85246	0.83403	7.227	8
D55	0.79365*	0.47543	7.613	9
D114	0.81250	0.75320	5.266	6
D121	0.85714	0.87594	10.439	13
D62	0.80952	0.83327	5.798	7
Avg	0.71783	0.70349	5.941	6.8

* 0.05 ** 0.01 ***0.001

Appendix S3. Observed heterozygosity (H_o), expected heterozygosity (H_e), allelic richness (A_R), and number of alleles (N_A) by locus for population VA3. Significant deviations from Hardy-Weinberg equilibrium are denoted with asterisks.

VA4

Locus	H_o	H_e	A_R	N_A
B91	0.62500	0.51613	2.000	2
B08	0.93750	0.86492	6.920	7
D93	0.56250	0.58266	5.000	5
A18	0.81250	0.74798	4.994	7
D87	0.75000	0.78024	8.689	9
B67	0.50000	0.51613	2.000	2
D90	1.00000	0.85282	9.603	10
D55	1.00000	0.90524	9.757	10
D114	0.81250	0.80242	6.763	7
D121	0.87500	0.89113	10.757	11
D62	0.81250	0.79234	5.920	6
Avg	0.78977	0.75018	6.582	6.7

* 0.05 ** 0.01 ***0.001

Appendix S3. Observed heterozygosity (H_o), expected heterozygosity (H_e), allelic richness (A_R), and number of alleles (N_A) by locus for population VA4. No loci were found to be out of HWE.

VA2

Locus	H_o	H_e	A_R	N_A
B91	0.55556	0.50162	2.000	3
B08	0.88889	0.84694	6.920	7
D93	0.48889	0.56829	5.000	4
A18	0.71111	0.69613	4.994	5
D87	0.84444	0.83620	8.689	9
B67	0.48889	0.48539	2.000	2
D90	0.84444	0.84270	9.603	10
D55	0.73333	0.87640	9.757	10
D114	0.80000	0.78427	6.763	7
D121	0.75556***	0.86142	10.757	11
D62	0.82222	0.82722	5.920	6
Avg	0.72121	0.73878	6.024	7.3

* 0.05 ** 0.01 ***0.001

Appendix S3. Observed heterozygosity (H_o), expected heterozygosity (H_e), allelic richness (A_R), and number of alleles (N_A) by locus for population VA2. Significant deviations from Hardy-Weinberg equilibrium are denoted with asterisks.

Locus Pair	*P*-value	Locus Pair	*P*-value
B91 x B08	0.660	D93 x D87	0.097
B91 x D93	0.670	D93 x B67	0.350
B91 x A18	0.272	D93 x D90	0.295
B91 x D87	0.755	D93 x D55	0.634
B91 x B67	1.00	D93 x D114	0.518
B91 x D90	0.290	D93 x D121	0.299
B91 x D55	0.100	D93 x D62	0.801
B91 x D114	0.078	A18 x D87	0.359
B91 x D121	0.884	A18 x B67	0.625
B91 x D62	0.455	A18 x D90	0.526
B08 x D93	0.069	A18 x D55	0.964
B08 x A18	0.002	A18 x D114	0.315
B08 x D87	0.191	A18 x D121	0.954
B08 x D67	0.837	A18 x D62	0.375
B08 x D90	0.305	D87 x B67	0.900
B08 x D55	0.670	D87 x D90	0.681
B08 x D114	0.264	D87 x D55	0.368
B08 x D121	0.065	D87 x D114	0.069
B08 x D62	0.468	D87 x D121	0.378
B08 x A18	0.042	D87 x D62	0.737
B67 x D90	0.048	D90 x D62	0.393
B67 x D55	0.308	D55 x D114	0.121
B67 x D114	0.666	D55 x D121	0.110
B67 x D121	0.949	D55 x D62	0.978
B67 x D62	0.637	D114 x D121	0.149
D90 x D55	0.290	D114 x D62	0.590
D90 x D114	0.081	D121 x D62	0.531
D90 x D121	0.028		

Appendix S4. Pairwise tests of linkage disequilibrium for all loci, based on 1000 permutations and an adjusted *P*-value of 0.00090.

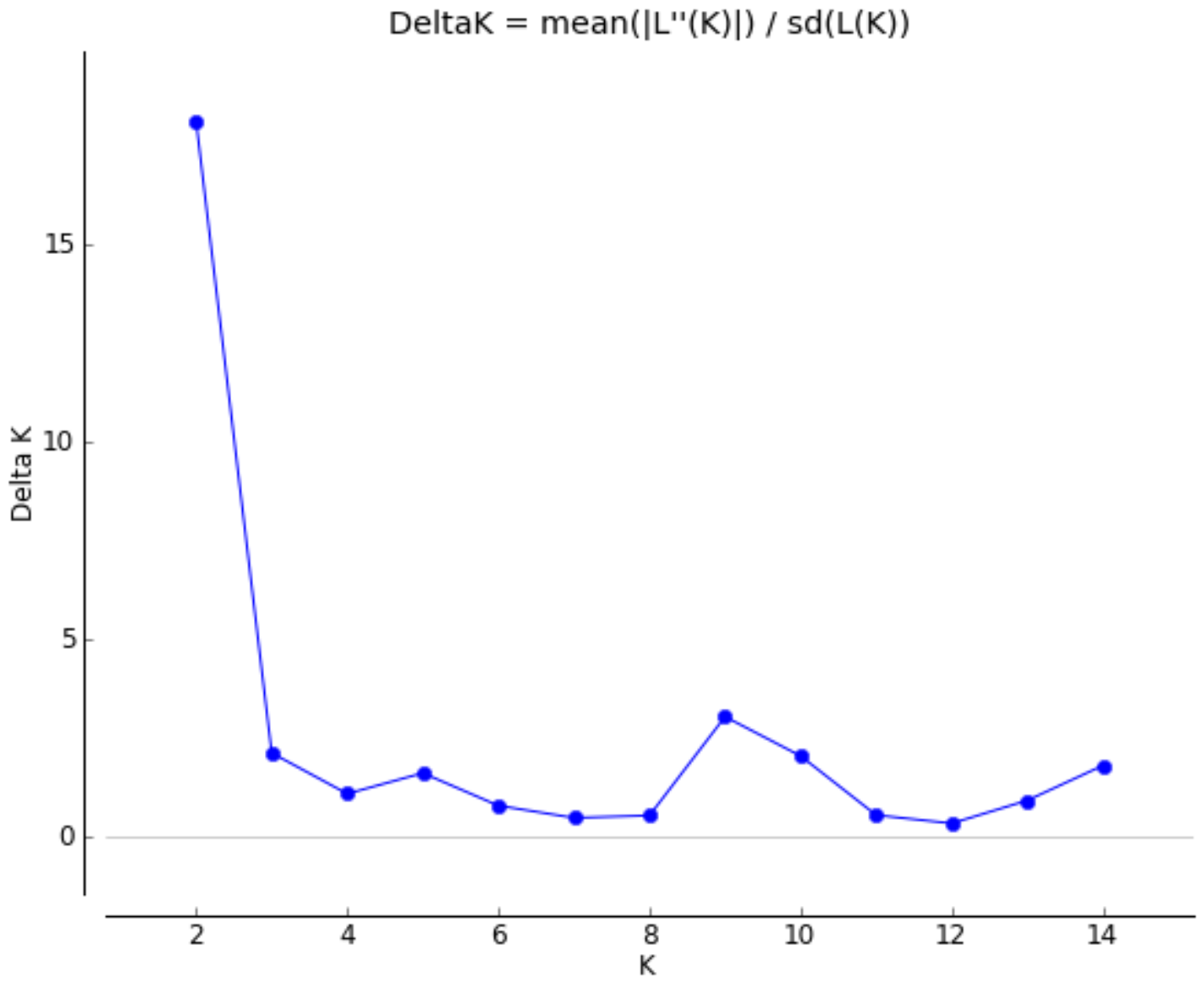

Appendix S5. ΔK plot under the Evanno method for the initial run of STRUCTURE finding the Patuxent River as a genotypic cluster

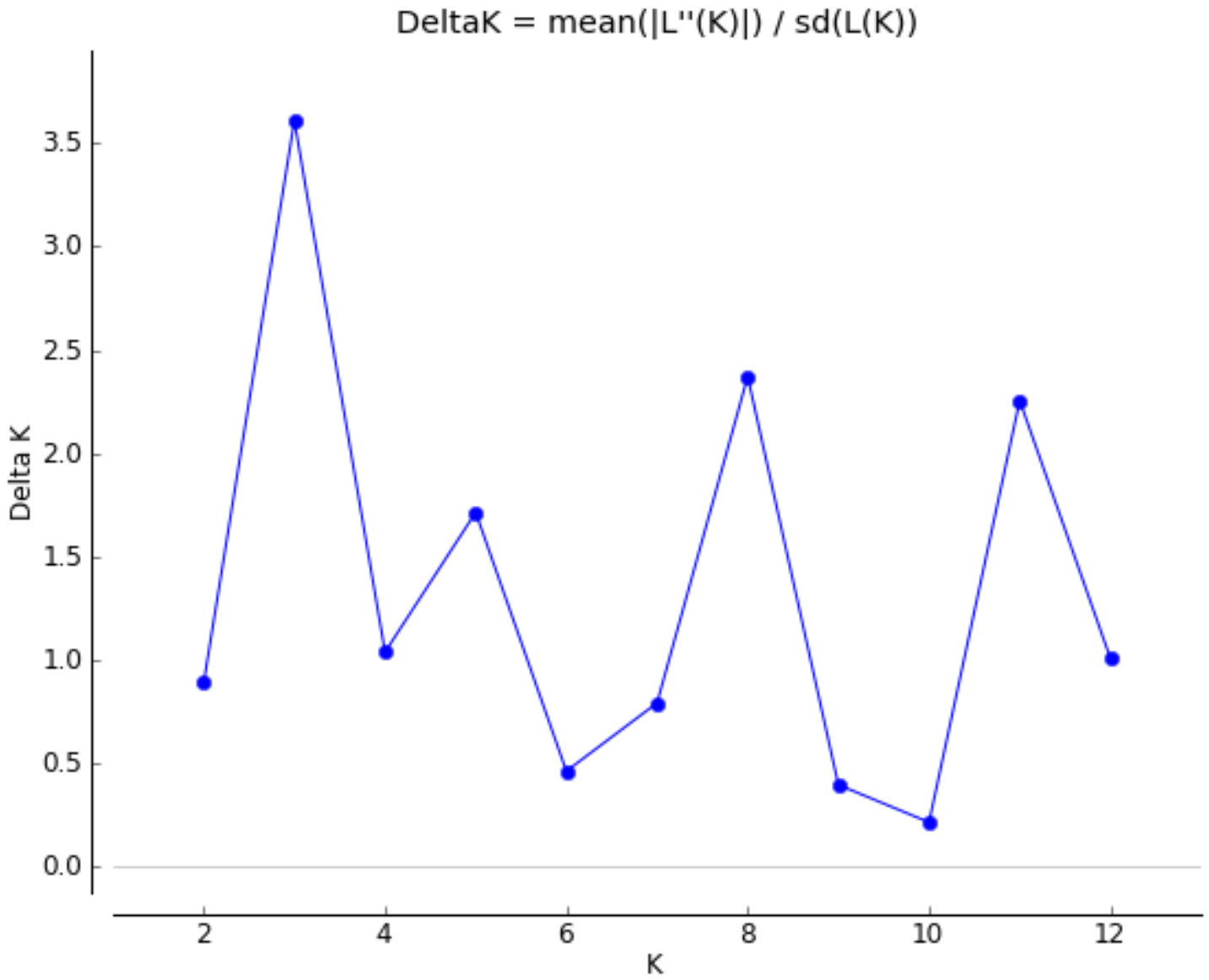

Appendix S5. ΔK plot under the Evanno method for the second run of STRUCTURE finding KI, ICB, and CoB as populations.

Variation Source	d.f.	Sum of Squares	Percent of Genetic Variation Explained	*P*-value
Sampling Locality				
Among Populations	14	22699.4	0.88	< 0.0001
Within Populations	1219	1146833.2	99.12	< 0.0001
Total	1233	1169532.6	100	
Bay Landscape				
Among Groups	2	8407.6	0.88	0.0154
Among Populations	12	14291.8	0.34	0.0808
Within Populations	1219	1146833.2	98.78	< 0.0001
Total		1169532.6	100	
STRUCTURE Cluster				
Among Groups	3	11321.4	0.96	0.0031
Among Populations	11	11378	0.13	0.3147
Within Populations	1219	1146833.2	98.91	0.0002
Total		1169532.6	100	

Appendix S6. AMOVA results indicating terrapin populations in Chesapeake Bay are weakly structured. Genetic data were partitioned by sampling locality, bay landscape (samples taken within tributary systems, Chesapeake Bay proper, and outside the bay), and by STRUCTURE cluster.

Population	TPM	SMM	Mode-shift
Kent Island	0.18	0.35	L-shaped
Patuxent River	0.12	0.42	L-shaped
Coastal Bay	0.45	0.71	L-shaped
Inner CB	0.48	0.90	L-shaped
Combined	0.65	0.94	L-shaped

Appendix S7. *P*-values for bottleneck detection under each model in BOTTLENECK. Parameters for the TPM include 95% step-wise mutations and a 12% variance on multi-step mutations. "L-shaped" distributions under a mode-shift test indicate a failure to detect a bottleneck. All results are based on 50,000 permutations. The bottom row represents the entire pooled dataset